Transport Properties of Single-File Water Molecules inside a Carbon Nanotube Biomimicking Water Channel

Guangchao Zuo, Rong Shen, Shaojie Ma, and Wanlin Guo*

Institute of Nano Science, Nanjing University of Aeronautics and Astronautics, Nanjing 210016, China

ARTICLE

ABSTRACT The single-file water transport through a biomimic water channel consisting of a (6,6) carbon nanotube (CNT) with different types of external point charges is studied using molecular dynamics simulations. It is demonstrated that, as in the aquaporins, asymmetrically positioned charges cannot generate robust unidirectional water flow in the CNT. Thermal fluctuation in bulk water competes with charge affinity to steer the water transport, resulting in nonmonotonic flow with intermittent reversal of transport direction. The energetic analysis suggests that the water−water interaction, determined by dipole orientation configuration, influences the transport rate significantly. These findings can provide correct biomimic understanding of water transport properties and will benefit the design of efficient functional nanofluidic devices.

KEYWORDS: transport property · carbon nanotube · water channel · free energy · molecular dynamics simulation

Water transport inside hydrophobic channels of carbon nanotubes (CNTs) represents a unique nanofluidic system,[1] which has broad prospects of technical applications, such as in hydroelectric power converters,[2,3] desalination of seawater,[4] and drug delivery.[5] In recent years, considerable attention has been devoted to bidirectional single-file water transport in both pristine and chemically modified CNTs, serving as prototypes for biological water channels. Various orientation and conduction properties of water in CNTs were detected, which can be modulated by exterior chemical modification,[6−8] structure deformation,[9] and smoothness of the interior surface[10−12] of CNTs, as well as external electrostatic field,[13,14] *etc*. Recently, Gong *et al.*[15] proposed by molecular dynamic simulations an intriguing concept for a molecular water pump, with three charges being asymmetrically positioned adjacent to a CNT, which was inspired by the charge distribution in biological water channels, aquaporins (AQPs), and showed a unique unidirectional flow resulting from an asymmetrical water-charge potential between two ends of the tube. This finding claimed a new way to design controllable nanofluidic devices. However, as has been established, AQPs can facilitate highly efficient and selectively passive permeation of water in response to osmotic gradient across cell membranes,[16] but cannot act as pumps or conduct water unidirectionally. In addition, water molecules in the pump design exhibit a bipolar orientation similar to that in AQPs, while Joseph and Aluru[17] pointed out that the flow direction is consistent with the dipole orientation of the water molecules in long CNTs. Therefore, it raises a fundamental question for such a proposed nanopump about the underlying mechanism and robustness of its ability to attain a unidirectional flow inside the CNT as prototypic AQPs, as it was suggested that the water molecules inside a CNT would strongly interact with other outside molecules when the CNT length was below 10 nm, and the interactions could greatly affect water conduction across the CNT.[17,18]

In this work, we observe reversible transport of single-file water molecules inside the CNT with a bias electrostatic potential induced by asymmetric charge distribution using molecular dynamics (MD) simulations, with a slight preference for the direction of the electric potential gradient within our simulation duration, in sharp contrast to the findings of Gong *et al.*[15] that water can be easily driven by external fields in a concerted fashion. The interactions of the transported water molecule with other water molecules inside and outside the CNT, together with the charges, play a critical role in the rate and direction of water conduction through the CNT, and the dipole orientation of water is unrelated to the flow direction in the CNT based on the length of aquaporins.

RESULTS AND DISCUSSION

For the MD simulations, the basic system termed "main+e" is presented in

*Address correspondence to wlguo@nuaa.edu.cn.

Received for review September 30, 2009 and accepted December 1, 2009.

Published online December 9, 2009.
10.1021/nn901334w

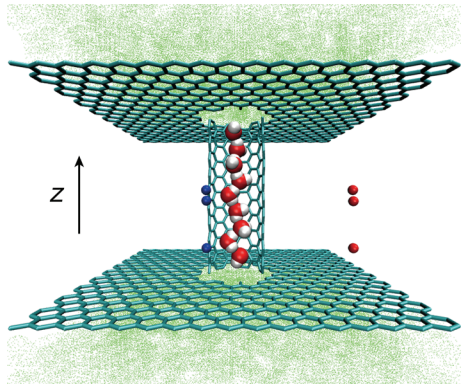

Figure 1. Overview of the main+e system. The carbon nanotube and graphite sheets are presented by cyan sticks. The blue spheres are the positive charges, and red spheres are the negative charges, while the electric quality is 0.5, 0.5, and 1.0e from top to bottom. Water molecules inside and outside the nanotube are rendered in vdW with oxygen in red and hydrogen in white and dotted representations, respectively.

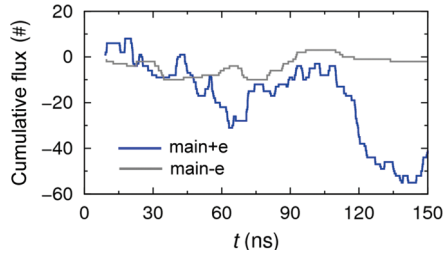

Figure 2. Cumulative flux of water molecules as a function of time for the main+e and main−e systems.

Figure 1 as in ref 15: a (6,6) CNT with a diameter of 8.1 Å and a length of 23.4 Å was embedded between two graphite sheets solvated by bulk water, which was centered at the Cartesian origin with its normal axis being along the *z* direction. Three positive charges with electric qualities of 1.0, 0.5, and 0.5e were positioned at $z = -8$, -0.7, and 0.7 Å, representing the polar residues Arg197, Asn194, and Asn78 in aquaporin-1 (AQP1),[19] respectively, and all of the positive charges were at the same radial distance (0.5 Å) from the carbon atoms. Three negative countercharges located at the same *z* coordinates were assigned close to the left side boundary of the system to keep the whole system electrically neutral. The positive charge at the bottom end was replaced by a negative charge (−1.0e) in the "main−e" system, while all of the charges were moved away in the "free" system. The CNT was modeled as uncharged Lennard-Jones atoms with parameters from ref 20. The TIP3P water model was used here.[21]

Figure 2 shows the cumulative flux of water molecules passing through the CNT in the main+e and main−e systems. The cumulative flux at time *t* is defined as the difference between the total numbers of water molecules that have crossed the CNT from bottom to top and the contrary direction. Our results yield various features of water transport, and the conclusions drawn here differ remarkably from the conclusions drawn by Gong *et al.*[15] We observe that (1) the cumulative flux variation over time is nonlinear; (2) the flow direction varies frequently with increasing simulation time; and thus (3) using the water-charge interaction alone to explain the results is insufficient.

During the last 145 ns of 150 ns simulation duration, 103 and 144 water molecules had penetrated the CNT along the *z* and $-z$ directions in the main+e system, respectively, resulting in a slight net flux of 0.28 water molecules per nanosecond, which is 1 order of magnitude lower than that observed in simulations of the same model by Gong *et al.*[15] To check whether the phenomenon was caused by the difference of the force fields used,[20] we performed simulations with the same parameters as Gong *et al.*[15] However, bidirectional conduction of water was also observed, although with a higher conduction rate. As the prototype of passive water channels,[22,23] the absence of net diffusion of the main+e system is expected in equilibrium MD simulations, which is actually the case. Lower conduction rate is observed in the main−e system, where only 21 and 23 water molecules had been conducted through the CNT along the *z* and $-z$ directions during the same duration, respectively. The net charge of a water molecule is zero, so its electrostatic interaction with a positive charge is similar to that with a negative charge, as shown in Figure 3a. So the lower conduction rate in the main−e system should be affected by other interactions. We thus turn to examine the water−water interaction and water−carbon interactions for both systems. The interaction energies of a water molecule in-

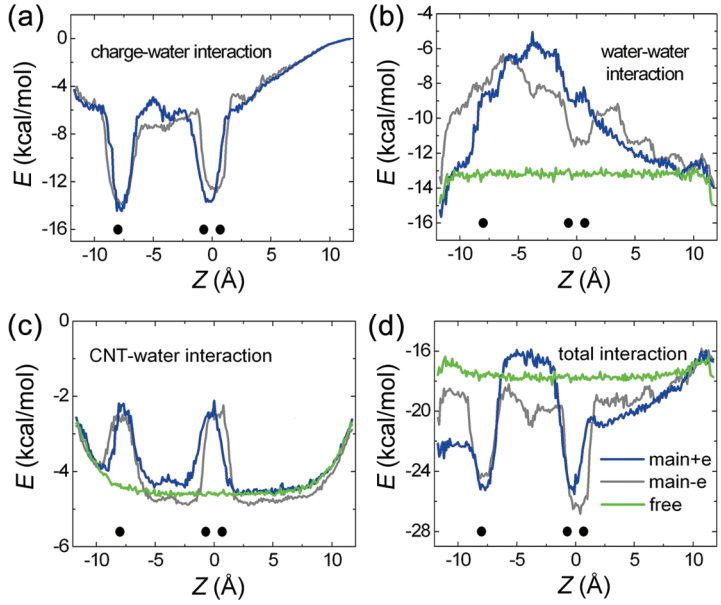

Figure 3. Interaction energy (kcal/mol) of a single-file water molecule at *z* with the (a) charges, (b) other water molecules, (c) CNT, and (d) total interaction by summing up preceding issues for the main+e system (blue), main−e system (gray), and free system (green). The black filled circles denote the locations of the charges.

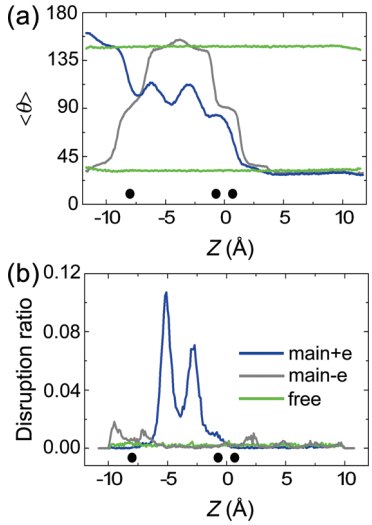

Figure 4. (a) Profile of $<\theta>$ along the nanotube, where $<\theta>$ is the average angle between a water dipole and the $+z$ direction. The black filled circles denote the locations of the charges in the main+e and main−e systems. (b) Disruption ratio of the water chain along the nanotube in the three systems.

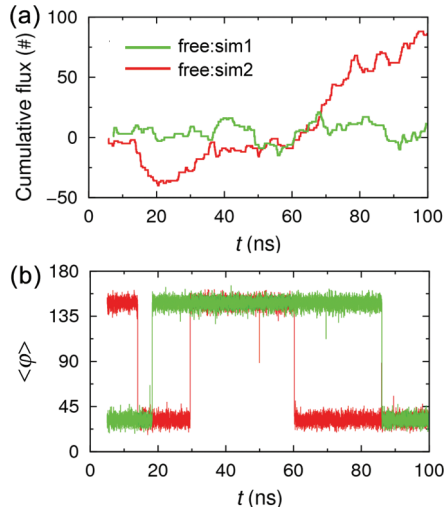

Figure 5. (a) Cumulative flux of water molecules as a function of time for the free system in two independent simulations. (b) Profile of $<\varphi>$ as a function of time, where $<\varphi>$ is the average of the angle between a water dipole and the $+z$ direction, and the average is taken over all of the water molecules inside the CNT.

side the CNT with other water molecules inside and outside the CNT, as well as with carbon atoms of the CNT, are calculated as shown in Figure 3b,c. The water−water interaction in the main+e system differs significantly from that in the main−e system, which is the main reason for the difference between the total interaction energies of a water molecule inside the CNT with its surroundings in the two systems, as shown in Figure 3d. The resulting barriers, referring to the difference between the maximum and minimum of the total interaction energy profile, for the main+e and main−e systems are 9.5 and 10.8 kcal/mol, respectively. In addition, the bias potential in the main−e system is smaller than that in the main+e system. As a result, water molecules are conducted more slowly in the main−e system than in the main+e system. For the free system, the water−water interaction holds at about −13 kcal/mol, which is significantly stronger than that in the two charged systems and the CNT−water interaction. Moreover, the total interaction energy profile of the free system is flatter than those of the main+e and main−e systems, thus resulting in faster water transport as will be discussed later.

To understand the mechanism underlying the difference in the water−water interaction between these systems, we examined the average dipole orientation of water molecules in the CNT (Figure 4a), as the dipole interaction between the water molecules plays an important role in the behavior of the single-file water chain.[24,25] In the free system, water molecules maintain their dipole orientations in a uniform direction[1,13] so as to optimize the water−water interaction energy, and the concerted orientation angle $<\theta>$ reverses intermittently from ~30 to ~150°, as shown in Figure 4a. While the water dipole orientation in the main+e system presents a bipolar feature,[15] as in AQPs which can permit proton exclusion and rapid water permeation.[26,27] The water dipole orientation even abruptly reverts twice in the main−e system, and the water molecule at the bottom end reorients to the z direction. We further examined the contribution of hydrogen bonding between neighboring water molecules inside the tube by analyzing a single-file disruption ratio $dr(z)$,[22] based on the distance between the oxygen atoms of any two adjacent water molecules, i and j visiting z:

$$dr(z) = \mathrm{NDWP}(z)/\mathrm{NWP}(z) \quad (1)$$

where z is the midpoint of the z positions of the two neighboring oxygen atoms, and NDWP(z) and NWP(z) are the total number of disrupted water pairs and the total number of water pairs, respectively. If the distance between the oxygen atoms of the i, jth water pair exceeded 3.5 Å (the position of the first minimum in the oxygen−oxygen radial distribution function of liquid water), the water chain was considered disrupted at z. The results are shown in Figure 4b. For all systems, disruption is very rare, indicating a tight hydrogen bonding in the nanotube. In the free system, the $dr(z)$ is smooth and low; this is consistent with the water−water interaction result shown in Figure 3b. Compared to the main−e system, the main+e system has a larger disruption ratio in the interval of ~ -6 Å $< z <$ ~1 Å, corresponding to a weaker water−water interaction in this region, as shown in Figure 3b. We can therefore suggest that the water−water interaction is mainly attributed to the hydrogen bonds and the dipole orientations of water molecules in the tube.

The cumulative flux of water in the free system is also calculated and shown in Figure 5a. During a 95 ns

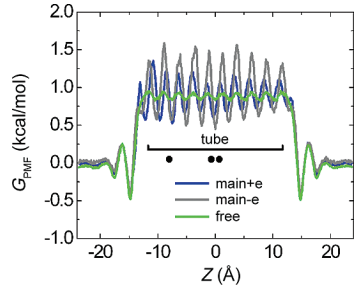

Figure 6. Free energy profiles for water permeating through the nanotube. The black filled circles denote the locations of the charges in the main+e and main−e systems.

duration, the net flux in the simulation sim1 approaches zero, while the upward flow in the simulation sim2 reveals a considerable advantage over downward flow. It is to be expected that at longer time scales the cumulative flux would fluctuate near the zero point. Notably, reversal of the flow direction becomes more frequent in the free system attributed to its lower potential barrier (Figure 3), and such reversal of the flow direction is suggested to be steered by thermal noise outside the CNT, which is unavoidable for any system in thermal contact with its surroundings.[28] In addition, Figure 5b shows that the orientations of single-file water molecules reverse collectively between two configurations and keep steady configuration for at least 10 ns, which is longer than the characteristic time (2−3 ns) for collective reorientations of single-file water molecules in a (6,6) CNT with a length of 13.4 Å.[1] It is clear that the longer the length of the water chain, the greater the barrier for the reorientation, thus the longer the time for flipping of the water chain.[17,24] It also shows that the water dipole orientation is unrelated to the water flow direction in the free system, in contrast to the direct correlation of them in a long CNT.[17]

Although there is a bias potential gradient between two ends of the tube, both the main+e and main−e systems show considerable permeation of water through the tube that is opposite to the potential gradient (Figure 2). To further understand the reversal of the direction of water transport in the CNT, we analyzed the potential of mean force (PMF) for water permeating through the CNT using

$$G_{PMG}(z) = -k_B T \ln[\rho(z)/\rho_0] \quad (2)$$

where $\rho(z)$ is the density of water molecules along the tube axis, within a distance of 4.1 Å from the axis, and ρ_0 is the bulk water density. We refer to the two directional flows as "upflux" and "downflux" along the z and $-z$ directions, respectively. Figure 6 displays the PMF profile for water molecules permeating through the CNT in the three systems. The free energy profiles show wavelike patterns inside the CNT and have two valleys close to both ends of the CNT, indicating distinct water density distributions inside the CNT and bulk water. The wavelike profiles of the PMFs, induced by the tight hydrogen bonding network inside the nanotube and nanoscale confinement,[25] directly relate to the solid-like property of confined water.[29] We have calculated the axial diffusion coefficient D_z of single-file water molecules in the tube for the systems. The D_z of the free, main+e, and main−e systems are 1.11×10^{-5}, 0.49×10^{-5}, and 0.10×10^{-5} cm^2/s, respectively, which are significantly lower than that of the bulk water (2.69×10^{-5} cm^2/s).[30] It is clear that the larger the free energy barrier, the lower the axial diffusion coefficient. In contrast to the free system, water molecules need to overcome an additional barrier prior to entering and leaving the CNT in the main+e and main−e systems, and the barriers inside the CNT are even larger, resulting in the lower water conduction rates in the two systems. Compared to the main−e system, the additional barrier at the bottom entrance is larger than that at the top entrance in the main+e system, so that water molecule penetration into the CNT from the bottom end is more difficult than from the top end. In accord with the cumulative flux results, the downflux is slightly larger than the upflux in the main+e system, as a result of the small difference between the heights of the barriers (only 0.23 kcal/mol), whereas in the main−e system the upflux and the downflux are almost the same and the unidirectional water flow vanishes completely. However, random thermal fluctuation may annihilate the slight difference of the wavelike free energy profile at two ends of the CNT in the above systems, implying poor control of unidirectional water transport by the constrained charges even in the elegant distribution as in biological water channels.

In future applications where multiple CNTs are used simultaneously, the water transport against the electrostatic potential may not be neglected yet, which will reduce the efficiency of unidirectional flow significantly. Water molecules confined to the nanotube of different diameters exhibit different behaviors.[18,30,31] It can be expected that different structures at the two entrances of the CNTs or hydrophilic modification at one end of the CNTs[32] may facilitate the control of the flow direction.

CONCLUSIONS

We have investigated the transport properties of single-file water molecules inside a (6,6) CNT with different types of external point charges by extensive molecular dynamics simulations. Although it shows more efficient transport in the biomimic CNT channel with the elegant charge distribution as in aquaporins than others, no obvious unidirectional flow is exhibited. That is because random local density and thermal fluctuations may annihilate the slight differences of the free energy profile at two ends of the CNT to steer the flow direction competitively. For the CNT channel with the same charge distribution but an opposite sign of the charge

at the bottom end, the local water−water interaction is strengthened by variation of the water dipole orientations and tighter hydrogen bonding network inside the CNT, which reduces the transport rate considerably, let alone unidirectional flow. Interestingly, the flow direction is independent of concerted water orientations in the CNT free from charges with a length comparable to that of the pore of water channels. It is important that, when MD simulations are calculated on such a tricky issue, different results may be yielded in different running events on the exact same modeling system, due to the statistical nature of the MD process at finite temperature. Our results show that the biomimic CNT channel has the same diffusion property as the mimicked biological water channels, rather than a pump.[15]

METHODS

All MD simulations were carried out using the program NAMD2[33] in the NPT ensemble with a time step of 2 fs. Periodic boundary conditions were applied in all directions. The electrostatic forces were calculated without cutoff, using the particle mesh Ewald (PME) method.[34] The van der Waals interactions were calculated with a smooth cutoff (8−10 Å). The Langevin dynamics was employed to control the temperature at constant 300 K, and the Nosé−Hoover Langevin piston method[35] was used to maintain the pressure at 1 atm. The graphite sheets and carbon atoms at two entrances of the CNT were fixed, while charges were constrained to their initial positions with spring constants of 200 kcal/mol. For confined water transport, it is not possible to extrapolate from accidental or short time behavior to longer time scales, so MD simulations were performed repeatedly to obtain credible features of water flow in the nanochannel, with the total simulation time up to 1 μs.

Acknowledgment. This work is supported by the National Basic Research Program of China (973 Program) (2007CB936204), National and Jiangsu Province NSF (30970557, 10732040, 10802037, BK2008042), and the NUAA Funds (No. BCXJ 08-02).

REFERENCES AND NOTES

1. Hummer, G.; Rasaiah, J. C.; Noworyta, J. Water Conduction through the Hydrophobic Channel of a Carbon Nanotube. *Nature* **2001**, *414*, 188–190.
2. Zhao, Y. C.; Song, L.; Deng, K.; Liu, Z.; Zhang, Z. X.; Yang, Y. L.; Wang, C.; Yang, H. F.; Jin, A. Z.; Luo, Q.; *et al.* Individual Water-Filled Single-Walled Carbon Nanotubes as Hydroelectric Power Converters. *Adv. Mater.* **2008**, *20*, 1772–1776.
3. Yuan, Q. Z.; Zhao, Y. P. Hydroelectric Voltage Generation Based on Water-Filled Single-Walled Carbon Nanotubes. *J. Am. Chem. Soc.* **2009**, *131*, 6374–6376.
4. Corry, B. Designing Carbon Nanotube Membranes for Efficient Water Desalination. *J. Phys. Chem. B* **2008**, *112*, 1427–1434.
5. Bianco, A.; Kostarelos, K.; Prato, M. Applications of Carbon Nanotubes in Drug Delivery. *Curr. Opin. Chem. Biol.* **2005**, *9*, 674–679.
6. Joseph, S.; Mashl, R. J.; Jakobsson, E.; Aluru, N. R. Electrolytic Transport in Modified Carbon Nanotubes. *Nano Lett.* **2003**, *3*, 1399–1403.
7. Raghunathan, A. V.; Aluru, N. R. Molecular Understanding of Osmosis in Semipermeable Membranes. *Phys. Rev. Lett.* **2006**, *97*, 024501.
8. Striolo, A. Water Self-Diffusion through Narrow Oxygenated Carbon Nanotubes. *Nanotechnology* **2007**, *18*, 475704.
9. Wan, R. Z.; Li, J. Y.; Lu, H. J.; Fang, H. P. Controllable Water Channel Gating of Nanometer Dimensions. *J. Am. Chem. Soc.* **2005**, *127*, 7166–7170.
10. Majumder, M.; Chopra, N.; Andrews, R.; Hinds, B. J. Nanoscale Hydrodymics: Enhanced Flow in Carbon Nanotubes. *Nature* **2005**, *438*, 44.
11. Whitby, M.; Quirke, N. Fluid Flow in Carbon Nanotubes and Nanopipes. *Nature Nanotechnol.* **2007**, *2*, 87–94.
12. Joseph, S.; Aluru, N. R. Why Are Carbon Nanotubes Fast Transporters of Water? *Nano Lett.* **2008**, *8*, 452–458.
13. Li, J. Y.; Gong, X. J.; Lu, H. J.; Li, D.; Fang, H. P.; Zhou, R. H. Electrostatic Gating of a Nanometer Water Channel. *Proc. Natl. Acad. Sci. U.S.A.* **2007**, *104*, 3687–3692.
14. Liu, L.; Qiao, Y.; Chen, X. Pressure-Driven Water Infiltration into Carbon Nanotube: The Effect of Applied Charges. *Appl. Phys. Lett.* **2008**, *92*, 101927.
15. Gong, X. J.; Li, J. Y.; Lu, H. J.; Wan, R. Z.; Li, J. C.; Hu, J.; Fang, H. P. A Charge-Driven Molecular Water Pump. *Nat. Nanotechnol.* **2007**, *2*, 709–712.
16. Arge, P. Aquaporin Water Channels (Nobel Lecture). *Angew. Chem., Int. Ed.* **2004**, *43*, 4278–4290.
17. Joseph, S.; Aluru, N. R. Pumping of Confined Water in Carbon Nanotubes by Rotation−Translation Coupling. *Phys. Rev. Lett.* **2008**, *101*, 064502.
18. Thomas, J. A.; McGaughey, A. J. H. Water Flow in Carbon Nanotubes: Transition to Subcontinuum Transport. *Phys. Rev. Lett.* **2009**, *102*, 184502.
19. Sui, H. X.; Han, B.-G.; Lee, J. K.; Walian, P.; Jap, B. K. Structural Basis of Water-Specific Transport through the AQP1 Water Channel. *Nature* **2001**, *414*, 872–878.
20. Zhu, F. Q.; Schulten, K. Water and Proton Conduction through Carbon Nanotubes as Models for Biological Channels. *Biophys. J.* **2003**, *85*, 236–244.
21. Jorgensen, W. L.; Chandrasekhar, J.; Madura, J. D.; Impey, R. W.; Klein, M. L. Comparison of Simple Potential Functions for Simulating Liquid Water. *J. Chem. Phys.* **1983**, *79*, 926–935.
22. Jensen, M. Ø; Tajkhorshid, E.; Schulten, K. Electrostatic Tuning of Permeation and Selectivity in Aquaporin Water Channels. *Biophys. J.* **2003**, *85*, 2884–2899.
23. de Groot, B. L.; Grubmüller, H. The Dynamics and Energetics of Water Permeation and Proton Exclusion in Aquaporins. *Curr. Opin. Struct. Biol.* **2005**, *15*, 176–183.
24. Pomes, R.; Roux, B. Free Energy Profiles for H^+ Conduction along Hydrogen-Bonded Chains of Water Molecules. *Biophys. J.* **1998**, *75*, 33–40.
25. Fang, H. P.; Wan, R. Z.; Gong, X. J.; Lu, H. J.; Li, S. Y. Dynamics of Single-File Water Chains inside Nanoscale Channels: Physics, Biological Significance and Applications. *J. Phys. D. Appl. Phys.* **2008**, *41*, 103002.
26. Tajkhorshid, E.; Nollert, P.; Jensen, M. Ø.; Miercke, L. J. W.; O'Connell, J.; Stroud, R. M.; Schulten, K. Control of the Selectivity of the Aquaporin Water Channel Family by Global Orientational Tuning. *Science* **2002**, *296*, 525–530.
27. de Groot, B. L.; Grubmüller, H. Water Permeation Across Biological Membranes: Mechanism and Dynamics of Aquaporin-1 and GlpF. *Science* **2001**, *276*, 2353–2357.
28. Astumian, R. D. Thermodynamics and Kinetics of a Brownian Motor. *Science* **1997**, *276*, 917–922.
29. Yuan, Q. Z.; Zhao, Y. P. Transport Properties and Induced Voltage in the Structure of Water-Filled Single-Walled Boron−Nitrogen Nanotubes. *Biomicrofluidics* **2009**, *3*, 022411.
30. Mashl, R. J.; Joseph, S.; Aluru, N. R.; Jakobsson, E. Anomalously Immobilized Water: A New Water Phase Induced by Confinement in Nanotubes. *Nano Lett.* **2003**, *3*, 589–592.
31. Koga, K.; Gao, G. T.; Tanaka, H.; Zeng, X. C. Formation of Ordered Ice Nanotubes Inside Carbon Nanotubes. *Nature* **2001**, *412*, 802–805.

32. Fornasiero, F.; Park, H. G.; Holt, J. K.; Stadermann, M.; Grigoropoulos, C. P.; Noy, A.; Bakajin, O. Ion Exclusion by Sub-2-nm Carbon Nanotube Pores. *Proc. Natl. Acad. Sci. U.S.A.* **2008**, *105*, 17250–17255.
33. Phillips, J. C.; Braun, R.; Wang, W.; Gumbart, J.; Tajkhorshid, E.; Villa, E.; Chipot, C.; Skeel, R. D.; Kalé, L.; Schulten, K. Scalable Molecular Dynamics with NAMD. *J. Comput. Chem.* **2005**, *26*, 1781–1802.
34. Essmann, U.; Perera, L.; Berkowitz, M. L.; Darden, T.; Lee, H.; Pedersen, L. G. A Smooth Particle Mesh Ewald Method. *J. Chem. Phys.* **1995**, *103*, 8577–8593.
35. Feller, S. E.; Zhang, Y. H.; Pastor, R. W.; Brooks, B. R. Constant Pressure Molecular Dynamics Simulation: The Langevin Piston Method. *J. Chem. Phys.* **1995**, *103*, 4613–4621.